IIETA International Information and Engineering Technology Association
Advancing the World of Information and Engineering

Annales de Chimie - Science des Matériaux
Vol. 50, No. 3, June, 2026, pp. 275-282
Journal homepage: http://iieta.org/journals/acsm

Corrosion Inhibition of AA6061 in Simulated Formation Water Using Orange Peel Extract

Saraa M. Mohammed[1*], Balsam M. Shaker[1], Mais A. Abdulkarem[2], Mohammed Ali Abdulrehman[2]

[1] Department of Construction and Projects, Mustansiriyah University, Baghdad 10045, Iraq
[2] Department of Materials Engineering, Mustansiriyah University, Baghdad 10045, Iraq

Corresponding Author Email: saraamajeed96@uomustansiriyah.edu.iq

https://doi.org/10.18280/acsm.500307

Received: 3 April 2026
Revised: 9 June 2026
Accepted: 17 June 2026
Available online: 30 June 2026

Keywords:
adsorption mechanism, aluminum alloy 6061, corrosion inhibition, orange peel extract, potentiodynamic polarization

ABSTRACT

This study aimed to investigate the inhibitive action of orange peel extract (OPE) on AA6061 subjected to artificial formation water by employing electrochemical and surface analytical techniques. The electrochemical investigation conducted through potentiodynamic polarization indicated a considerable reduction in corrosion current density (Icorr) and corrosion rate (CR) with increasing concentrations of OPE, achieving a maximum inhibition efficacy of 98.99% for 2.5% OPE concentration. The impact of temperature was assessed, and it was revealed that there was an increase in corrosion with increasing temperature; however, OPE was found to have significant inhibition efficacy, implying a good protective action. According to the Fourier-transform infrared spectroscopy (FTIR) analysis, there were oxygen-containing functional groups (-OH, C=O, and C-O) within the OPE, which facilitated adsorption. The scanning electron microscopy (SEM) images show considerable changes in the surface morphology, indicating the formation of a protective film. The reason for such inhibition is the adsorption of the active ingredients of OPE onto the AA6061 alloy surface. The fact that the inhibition effectiveness decreases as the temperature increases means that there is a possibility of physisorption. The results indicate that OPE can be a sustainable and green corrosion inhibitor for industrial use, particularly in cases where the inhibitor is directly injected into corrosive media.

1. INTRODUCTION

These include direct introduction into the fluid flow. The degradation of metallic materials, specifically aluminum alloy 6061 (AA6061), is a common issue in various industrial areas, including the oil and gas, marine, and transport sectors. Although AA6061 is widely used because of its excellent strength-to-weight ratio and intrinsic corrosion resistance, this material is still prone to specific corrosion modes, particularly the localized type induced by a chlorinated environment, such as simulated formation water [1-3]. Such degradation significantly reduces the service life and reliability of metallic parts. Consequently, there is a need to develop a reliable corrosion protection strategy [4, 5]. In these industrial processes, inhibition is usually achieved by continuously introducing an inhibitor into the fluid flow. Conventional corrosion inhibitors are commonly used to address this issue. However, most of these materials are synthesized chemicals that are often harmful to the environment and living organisms, which limits their widespread use [2, 6]. Growing awareness of environmental protection-related concerns has resulted in an increased interest in research on substances that do not harm nature. As far as environmentally friendly corrosion inhibitors are concerned, plant extracts appear to be a suitable choice owing to their natural nature, lower toxicity, cost efficiency, and abundance. Plant extracts contain an array of biologically active substances, including flavonoids, alkaloids, tannins, and organic acids. All of these substances contain heteroatoms (oxygen and nitrogen) and conjugated π-electronic systems that make the process of adsorption highly efficient [7-9]. From all the extracts of plants, citrus products, particularly orange peel extract (OPE), have received great popularity owing to their high polyphenol concentration, as well as oxygen-containing functional groups that enable the formation of stable bonds with metal surfaces [3, 4]. Such components are tasked with creating a layer to prevent corrosive substances from contacting the metal surface [6, 10].

Among the main factors responsible for the inhibition action of corrosion inhibitors are adsorption processes, which may be carried out both physically and chemically [9, 11]. At present, electrochemical approaches appear to be among the most widespread means of research into the behavior of materials and analysis of inhibitor efficacy. The electrochemical study provides information on important parameters such as corrosion current density (Icorr) and polarization resistance. The electrochemical investigation of the inhibitory activity was supplemented by different methods for the analysis of the metal surface morphology and composition. Approaches such as scanning electron microscopy (SEM), Fourier-transform infrared spectroscopy (FTIR), and energy-dispersive X-ray spectroscopy provide valuable data about the distribution of different functional groups and chemical elements in the

studied samples [12-14]. In addition, the latest trends in the field prove the need to combine experiments and calculations when investigating the process of adsorption [11, 12].

Inhibitor efficiency is affected by several parameters, including inhibitor concentration, temperature, immersion period, and composition of the corrosive medium. For instance, an increased inhibitor concentration improves the adsorption performance, whereas increasing the temperature might decrease the inhibition efficiency because of the desorption phenomenon [10, 15]. Artificial formation water environments are highly complicated and diverse owing to the presence of many different ions in such media. As a result, the investigation of corrosion mechanisms in this type of media becomes more challenging [15, 16]. Many advancements have been made regarding this issue, yet the existing literature provides no complete insight into the adsorption-inhibition properties of OPE in relation to AA6061 within simulated formation-water environments. First, all previous studies dealing with this subject matter were conducted with other aluminum alloys or extracts of various plants. Moreover, the literature review indicated the absence of studies investigating OPE inhibition from the perspective of electrochemical and surface analyses [16, 17].

To the best of our knowledge, not many studies have been devoted to the combination of electrochemical measurements with surface studies, which would provide a complete understanding of the mechanisms of adsorption and corrosion inhibition properties of the studied extract in simulated formation water for AA6061. The main purpose of this research was to perform a mechanistic study of the adsorption and corrosion inhibition properties of OPE on AA6061 in simulated formation water. Traditionally, corrosion resistance has been obtained by applying protective coatings to materials. In contrast, the novelty of the proposed approach is the addition of a green corrosion inhibitor to the corrosive medium. In this case, a protective layer is spontaneously created by the inhibitor molecules through adsorption mechanisms. The suggested approach resembles industrial practices in which corrosion inhibitors are constantly added to the stream using dedicated injection equipment. In this manner, the pipeline, tank, or unit is protected during operation under flow conditions. Thus, this study assessed the corrosion inhibition effectiveness of OPE in synthetic formation water through electrochemical and surface studies conducted in a laboratory setting. This will help understand the mechanism of inhibitor adsorption and protection of the AA6061 aluminum alloy. In this case, the potential of the proposed technology increases significantly because OPE can serve as a natural inhibitor that can substitute synthetic ones in the industry [18-20].

2. METHODOLOGY

AA6061 aluminum alloy was selected as the substrate material in this study because of its extensive usage in industry and susceptibility to localized corrosion in the presence of chloride ions. The composition of the alloy was confirmed via the analysis performed by optical emission spectroscopy in accordance with existing standard criteria. AA6061 specimens were machined into cylindrical pieces measuring 2 mm in thickness and 50 mm in diameter. During the preparation process, the specimens were mechanically polished using silicon carbide abrasive papers of various grades, up to 1200. They were subsequently washed in distilled water and degreased with an acetone solution.

The preparation of OPE requires an effective and straightforward technique that is very reliable. Fresh peels from oranges were first washed in distilled water and dried for three days in sunlight. These peels were then ground into a fine powder and passed through a sieve to collect particles of less than 300 μm. Orange powder weighing 100 g was mixed with 1000 mL of ethanol and water in a ratio of 80:20 v/v and extracted by reflux or fractional distillation for 1 h. This extract was filtered through filter paper and stored at 4 °C in a fridge.

A mixture of formation water was developed under harsh environmental conditions. Analytical salts were mixed with deionized water to make the following solutions: NaCl (35 g/L), $MgCl_2 \cdot 6H_2O$ (7 g/L), Na_2SO_4 (3.5 g/L), $CaCl_2 \cdot 2H_2O$ (1.1 g/L), KCl (0.7 g/L), and $NaHCO_3$ (0.2 g/L). The electrolyte solutions were tested under laboratory conditions, which were not deaerated but had a natural air content. To prepare for each test, the pH was standardized between 8.0 and 8.2 with dilute HCl or NaOH and checked using the calibrated pH meter. This is because fresh electrolyte solutions were prepared before conducting any tests to prevent pH changes.

In this study, the OPE was added to the corrosive environment in dissolved form as a corrosion inhibitor without creating any barrier between the metal surface and the corrosion medium. This method was used to analyze the behavior of this compound in electrolytic environments. Electrochemical analyses of the AA6061 specimens were carried out using a three-electrode cell setup connected to a potentiostat/galvanostat (Gamry G300). The AA6061 alloy sample acted as the working electrode, while a graphite rod was used as the counter electrode. A saturated calomel electrode (SCE) was selected as the reference electrode. Before the electrochemical experiments, the specimens were exposed to the test solution for 60 min to permit the interaction of the corrosion inhibitor molecules with the metal surface. Then, the working electrode was allowed to rest at the open circuit potential (OCP) for 30 min prior to potentiodynamic polarization studies. Electrochemical investigations were repeated three times, and the results are reported as the mean ± standard deviation (SD) values. Polarization was performed at both 25 °C and 50 °C. Potentiodynamic polarizations were performed using a scan rate of 1 mV s^{-1} in a potential window of ±250 mV with respect to the OCP. There was no IR compensation for the polarization. The polarization data were analyzed using the Gamry Framework. The Ecorr and Icorr values were obtained using Tafel extrapolations from the linear regions on the anodic and cathodic sides of the polarizations and Tafel slopes. Inhibition efficiencies and surface coverages were then calculated using the Icorr.

Moreover, to elucidate the nature of the interaction of the inhibitor with the metal surface, several surface characterization techniques were employed. The adsorption of the inhibitor onto the metal surface was investigated by FTIR, where spectra were acquired at certain wavenumber ranges, and certain characteristic peaks belonging to OH, C=O, and other oxygenated functional groups were identified. Further, the surface morphology was analyzed by SEM for the comparison of corroded and uncorroded surfaces, both in the absence and presence of the inhibitor. In this study, the effect of the concentration and temperature of the inhibitor on the corrosion of AA6061 was investigated. These parameters were chosen as illustrative examples of variations that could occur

in industry to evaluate the influence of inhibitor concentration and temperature on the corrosion behavior of AA6061 in simulated formation water.

3. RESULTS AND DISCUSSION

3.1 Potentiodynamic polarization analysis

As can be seen from the potentiodynamic polarization curves (Figure 1) and the data listed in Table 1, there was a pronounced increase in the corrosion resistance with increasing concentrations of OPE. It should be noted that according to Figure 1, with an increase in the OPE content, the current densities of both the anodic and cathodic branches decreased.

Table 1. Corrosion current density (Icorr) and corrosion rate (CR) of AA6061 at different orange peel extract (OPE) concentrations

Concentration (%)	Icorr (mA/cm²)	CR (mm/year)
0 (Blank)	0.296 ± 0.011	0.00323
1	0.103 ± 0.005	0.00112
1.5	0.063 ± 0.004	0.00069
2	0.029 ± 0.002	0.00032
2.5	0.003 ± 0.0001	0.00003
3	0.011 ± 0.001	0.00012

Note: CR = corrosion rate.

The Icorr decreased from 0.296 to 0.003 mA/cm² at a concentration of 2.5%, indicating the strong effect of OPE in reducing the corrosion process. In support of this conclusion, the corrosion rate (CR) calculated in accordance with Table 1 showed a decrease from 0.00323 mm/year in the blank solution to 0.000033 mm/year with 2.5% OPE.

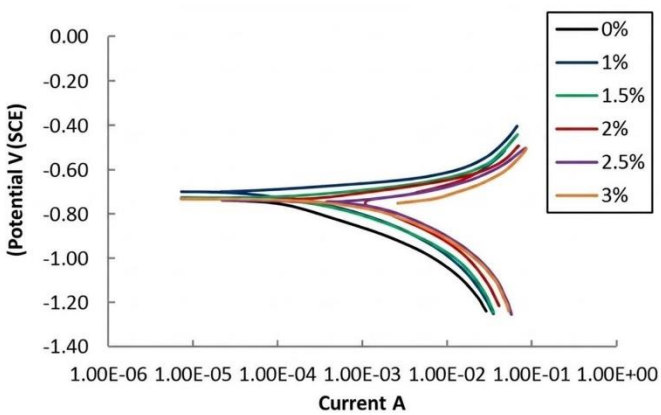

Figure 1. The potentiodynamic polarization curves of AA6061 at different orange peel extract (OPE) concentrations (0–3 wt. %)

From Figure 1, it can be concluded that the increasing reduction in the current density, depending on the concentration of inhibitors, is associated with their effectiveness in reducing the transfer of charge. The inhibition efficiency (IE%) increased significantly with increasing OPE concentration, ranging from 65.20% at 1% to 78.72% at 1.5%, up to a maximum of 98.99% at the optimum concentration of 2.5%. Figure 1 shows that the highest IE% was associated with the lowest current density. Such results can be attributed to the more complete filling of the aluminum surface owing to adsorption, with a high surface coverage ($\theta \approx 0.99$), which leads to the blocking of the active areas of corrosion. Thus, at concentrations below the optimal level, surface coverage was insufficient. With an increase in the OPE content to 3% (see Figure 1), the opposite tendency was observed. An increase in the Icorr was accompanied by a decrease in the inhibition efficiency to 96.28% and a CR increase to 0.00012 mm/year, suggesting that the inhibitor concentration becomes too high and, as a result, creates a poorly compacted protective layer.

In addition, it should be noted that the corrosion potential (Ecorr) changes slightly and varies from -691 mV to -711 mV (less than 20 mV) in accordance with Figure 1, showing that the OPE has a pronounced mixed effect on both the cathodic and anodic reactions of the process. Thus, as shown in Figure 1, the addition of a natural inhibitor does not fundamentally alter the corrosion mechanism [2, 19]. Based on the results obtained from Figures 1 and 2, it can be stated that the inhibition efficiency of OPE is significantly affected by its concentration in the solution. This means that the adsorption effect plays the most important role in controlling corrosion processes.

3.2 Effect of inhibitor concentration

The CR of AA6061 depends significantly on the concentration of OPE. This is demonstrated by the electrochemical data analyzed in Section 3.1. A significant drop was noted in the Icorr with increasing inhibitor concentration. This corresponds to a substantial decrease in the CR. In addition, the CR also decreased substantially, ranging from 0.00323 mm/year for the blank solution to 0.000033 mm/year at 2.5% OPE.

Moreover, the inhibition efficiency (IE%) gradually increased depending on the inhibitor concentration. A maximum IE of 98.99% was recorded at 2.5% OPE concentration, which was considered the optimum concentration level. This high performance was due to the increased adsorption of phytochemicals contained in the extract, which provided improved surface coverage ($\theta \approx 0.99$) and efficient inhibition of active corrosion sites. Therefore, an efficient protective film was established, forming a physical barrier that hindered chloride ion diffusion into the simulated formation fluid.

IE values of 65.20% at 1% OPE and 78.72% at 1.5% were recorded, corresponding to higher CRs. As a result, there is low coverage of surface sites, leading to inadequate surface protection. In contrast, 96.28% IE at 3% OPE was noted, along with a marginal CR of 0.00012 mm/year, indicating the formation of an unstable adsorption layer when the optimum inhibitor concentration was exceeded.

Additionally, the increasing efficiency with increasing OPE concentration confirms that the process of inhibition is adsorption-controlled. An increase in the inhibitor concentration leads to a higher concentration of adsorbed molecules [3, 7]. The adsorption of the inhibitor was limited by the saturation point, after which the added inhibitor molecules had little or no effect on the process. Moreover, excess OPE leads to a less stable film [9].

In summary, the effectiveness of inhibition was highly dependent on the inhibitor concentration, with 2.5% being the optimum concentration.

3.3 Effect of temperature

The corrosion of AA6061 at different temperatures in artificial formation water was determined through potentiodynamic polarization studies with and without the addition of OPE. As depicted in Figures 2 and 3, the obtained results were used to determine their values, which are presented in Table 2.

Table 2. Potentiodynamic polarization parameters of AA6061 at different temperatures

Condition	Temp. (°C)	Icorr (mA/cm²)	CR (mm/year)	IE (%)
Blank	25	0.296 ± 0.009	0.00323 ± 0.00010	—
2.5% OPE	25	0.0030 ± 0.0001	0.00003 ± 0.000001	98.99 ± 0.14
Blank	35	0.512 ± 0.015	0.00558 ± 0.00017	—
2.5% OPE	35	0.0087 ± 0.0003	0.00009 ± 0.000003	98.30 ± 0.22
Blank	45	0.891 ± 0.027	0.00971 ± 0.00029	—
2.5% OPE	45	0.0239 ± 0.0007	0.00026 ± 0.000008	97.32 ± 0.30
Blank	50	1.623 ± 0.049	0.01769 ± 0.00053	—

Note: OPE = orange peel extract; CR = CR = corrosion rate; IE = inhibition efficiency

Without OPE (Figure 2), Icorr increased sharply when the temperature was increased from 25 °C to 50 °C. Specifically, Icorr increased from 0.296 mA/cm² at 25 °C to 1.623 mA/cm² at 50 °C. The increase in Icorr is associated with an increase in CR from 0.00323 mm/y at 25 °C to 0.01769 mm/y at 50 °C, indicating that an increase in temperature enhances the corrosion process. According to Figure 2, the cathodic and anodic branches tend to move towards higher current densities with an increase in temperature. This can be explained by electrochemical reactions that become faster at elevated temperatures owing to the enhanced ionic mobility and charge transfer rate [21].

With 2.5% OPE (Figure 3), the Icorr and CR decreased remarkably in all temperature ranges studied. At 25 °C, Icorr dropped drastically to 0.0030 mA/cm² with a CR of only 0.000033 mm/yr. As the temperature increased to 50 °C, Icorr increased progressively to 0.0759 mA/cm², and CR increased to 0.00083 mm/year. As shown in Figure 3, despite an increase in the current density at all temperatures considered, there was no drastic change, similar to the case of the blank solution, proving the excellent inhibition performance of the OPE.

An increase in CR with increasing temperature in the presence of an inhibitor implies a decrease in the inhibition efficacy. This occurred because of the tendency of the inhibitor molecules to desorb from the AA6061 surface at high temperatures. When the temperature rises, the adsorption-desorption equilibrium tends to favor desorption, thereby reducing the amount of inhibitor molecules present. Thus, the inhibition was less effective owing to the weaker protective layer. Given the effect of temperature on inhibitive efficiency, one can infer that physisorption is likely involved in the adsorption phenomenon, considering that species adsorbed through physisorption can easily be desorbed due to increased temperatures.

The corrosion potential (Ecorr) did not show any significant variation with a change in temperature in either case, as shown in Figures 2 and 3. Therefore, this proves that the inhibition works in both directions; namely, it inhibits both anodic and cathodic reactions without changing the fundamental mechanism of the electrochemical reactions. Although the inhibition becomes less effective at higher temperatures, corrosion inhibition is still effective because some of the inhibitor molecules are strongly adsorbed on the surface of AA6061.

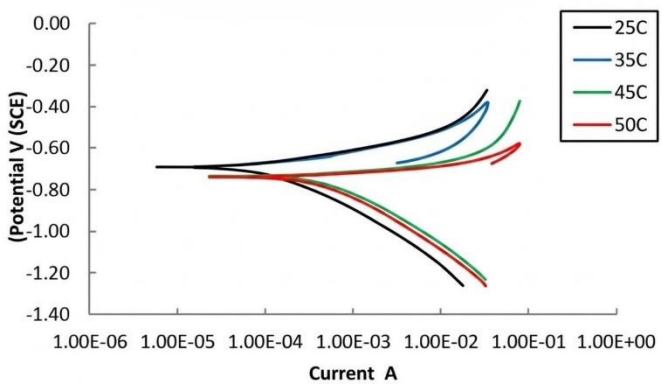

Figure 2. The potentiodynamic polarization curves of AA6061 in simulated formation water (blank) at different temperatures (25–50 °C)

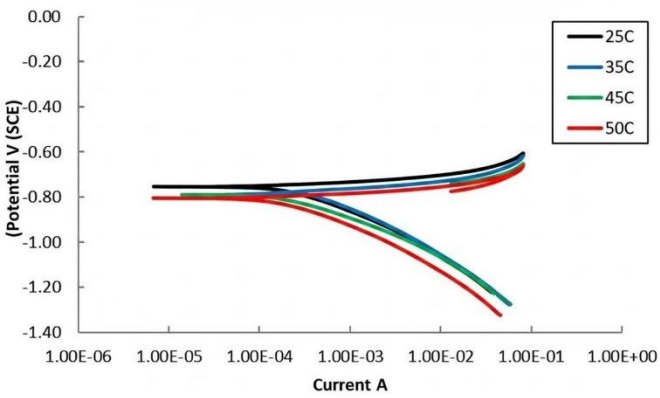

Figure 3. Potentiodynamic polarization curves of AA6061 in simulated formation water containing 2.5% orange peel extract (OPE) at different temperatures (25–50 °C)

3.4 Fourier-transform infrared spectroscopy analysis

The FTIR spectra shown in Figure 4 clearly indicate the types of functional groups and their interactions with the AA6061 surface following adsorption, which contribute significantly to the corrosion inhibition properties of the OPE. The FTIR spectrum of the OPE prior to adsorption on the alloy surface revealed several absorption bands corresponding to different functional groups, including –OH, aliphatic C-H, C=O, C=C, and C-O. A wide absorption band observed at 3200-3500 cm^{-1} relates to O-H stretching, implying the presence of hydroxyl groups attached to polyphenols and organic acids in the studied substance. Absorption peaks in the range from 2850 to 2950 cm^{-1} are associated with aliphatic C-H stretch vibrations. The strong peak near 1700 cm^{-1} denotes C=O stretch vibrations, proving the presence of a carbonyl functional group. Vibrations within the region of 1500-1600 cm^{-1} correspond to C=C stretch vibrations of aromatic

compounds, while peaks within the range of 1000-1300 cm^{-1} relate to C-O stretch vibrations.

Upon adsorption onto the AA6061 surface (Figure 4), changes in the intensity and shifts of the characteristic peaks can be easily observed. Specifically, there were reductions in the intensity and minor changes in the wavelength position of the O-H and C=O absorption peaks. Thus, these functional groups appeared to be directly involved in the adsorption process on the AA6061 surface. These results indicate the existence of strong interactions between the functional groups and the aluminum surface via donor-acceptor interactions or electrostatic attraction. Oxygen-containing functional groups increase the capacity of the substance to donate electron pairs and establish coordination with aluminum ions. As a result, a protective layer that blocks the active corrosion sites and minimizes the charge transfer processes is formed. Changes in the FTIR spectrum indicate the prevalence of the adsorption process in terms of the main mechanism of corrosion inhibition. Moreover, the predominance of oxygen-containing groups, such as hydroxyl and carbonyl groups, suggests the essential role of the polyphenolic and organic acid components. The high affinity for the metal surface contributed to the formation of a tight, firmly attached, and stable protective film. In conclusion, the FTIR findings indicate that oxygen-containing species from the OPE are adsorbed onto the surface of AA6061. The adsorption of this protective film could play a role in decreasing the Icorr and CR.

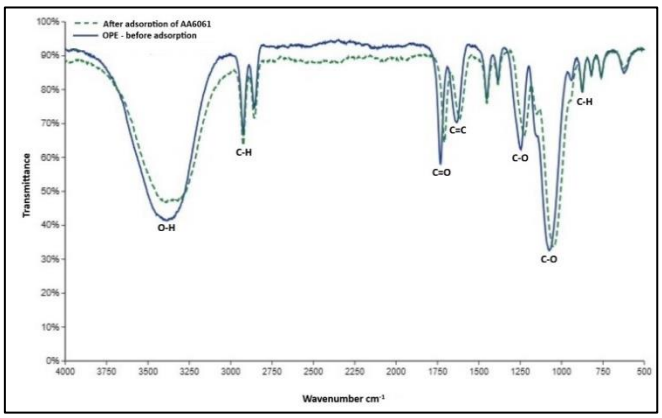

Figure 4. Fourier-transform infrared spectroscopy (FTIR) spectra of orange peel extract (OPE) before adsorption and after adsorption on the AA6061 surface

3.5 Scanning Electron Microscope analysis

The SEM technique was used to investigate the surface morphology of AA6061 samples under varied conditions (Figures 5–7). In the blank test condition, the AA6061 sample (Figure 5), when exposed to simulated formation water, exhibited severe surface damage through pitting corrosion, irregular surface roughness, and formation of corrosion products. As clearly demonstrated in Figure 5, the sample surface was highly heterogeneous, with pits and uneven surfaces. This indicates severe corrosive attacks on the sample surface owing to aggressive chlorides.

In contrast, the AA6061 sample exposed to the optimum concentration of OPE (Figure 6) showed a marked improvement in surface morphology, with a smoother surface with reduced pits and roughness on the surface. It can be clearly seen in Figure 6 that there is evidence of a continuous film formation on the surface, resulting in the protection of the surface from aggressive chloride attacks. This was mainly due to the formation of a protective film on the surface as a result of the adsorption of active compounds present in the OPE.

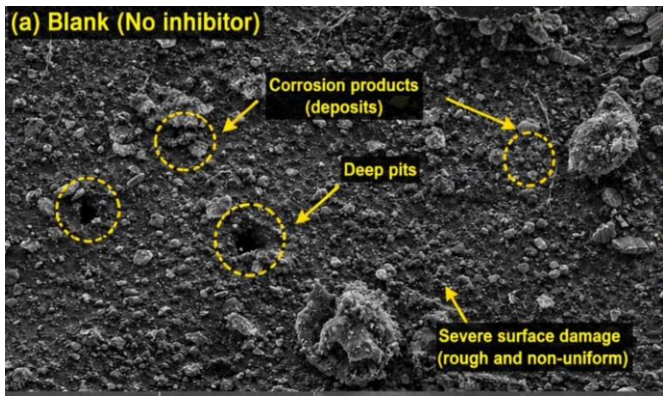

Figure 5. Scanning electron microscopy (SEM) images of the AA6061 surface in simulated formation water (blank condition)

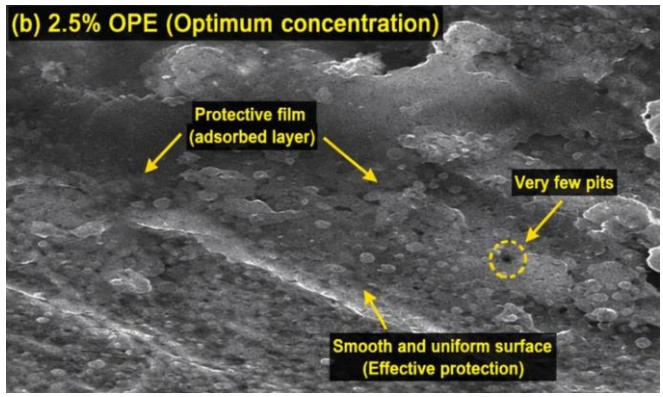

Figure 6. Scanning electron microscopy (SEM) image of the AA6061 surface in the simulated formation water containing 2.5% orange peel extract (OPE)

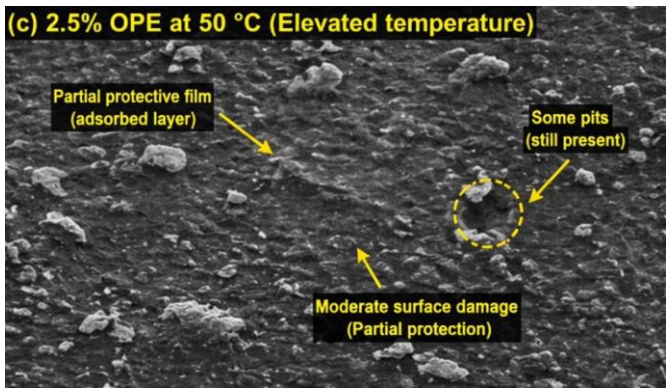

Figure 7. The scanning electron microscopy (SEM) image of the AA6061 surface in simulated formation water containing 2.5% orange peel extract (OPE) at 50 °C

At increased temperatures (Figure 7), partial deterioration of the surface film was observed. This can be observed in Figure 7, where there were still traces of pits and unevenness on the surface despite exposure to the inhibitor at the optimum concentration. At higher temperatures, partial decomposition occurs, leading to surface deterioration. This was due to the

thermal desorption of the inhibitor from the surface at high temperatures. Hence, there was partial deterioration of the protective layer in Figure 7 compared to that in Figure 6. Therefore, the existence of a protective adsorbed layer in Figure 6 and the partial deterioration of the layer in Figure 7 confirm that the adsorption mechanism is responsible for corrosion inhibition. The protective film serves as a physical barrier that separates the metallic surface from the corrosive electrolytes, preventing further corrosion.

The SEM images are consistent with the findings from electrochemical studies, where there was a marked reduction in the Icorr and CR, with decreased inhibition efficiency at increased temperatures.

3.6 Energy-dispersive X-ray spectroscopy analysis

The energy-dispersive X-ray spectroscopy (EDS) analysis of the AA6061 surface subjected to various environments is shown in Figures 8–10. The blank sample had a high concentration of aluminum and some chloride ions owing to its reaction with the corrosive environment.

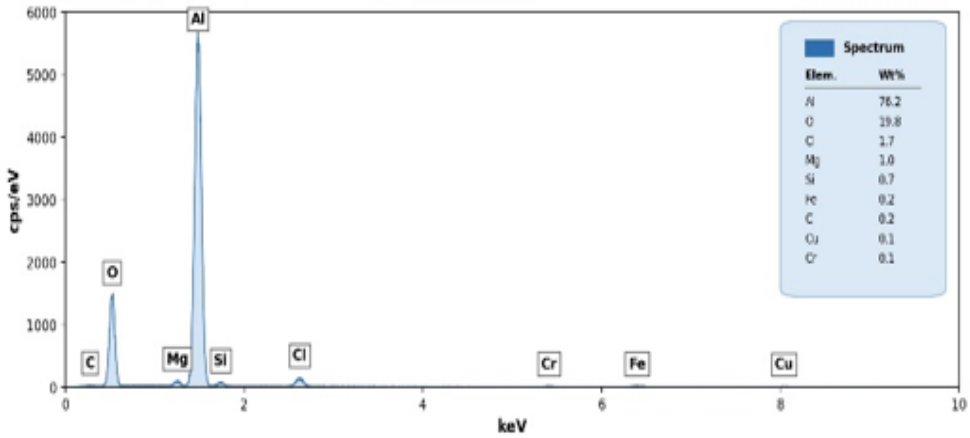

Figure 8. Energy-dispersive X-ray spectroscopy (EDS) analysis of AA6061 alloy sample exposed to simulated formation water without orange peel extract (OPE)

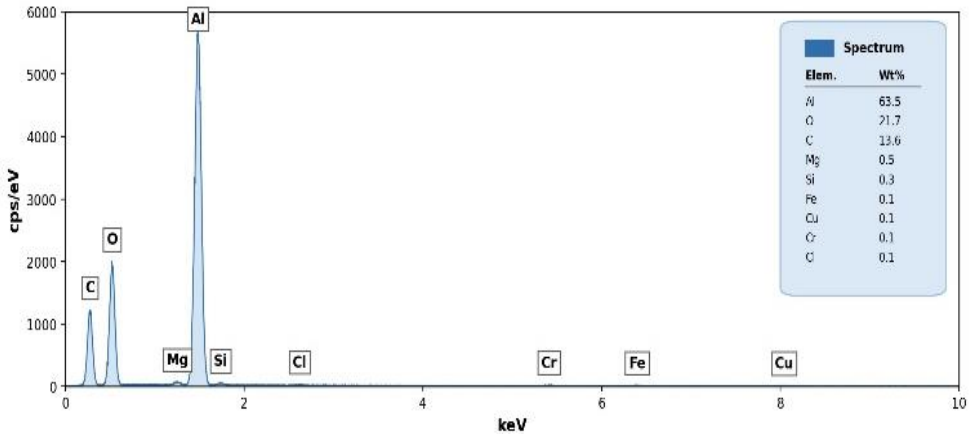

Figure 9. Energy-dispersive X-ray spectroscopy (EDS) analysis of AA6061 alloy sample exposed to simulated formation water with 2.5% orange peel extract (OPE) concentration at 25 ℃

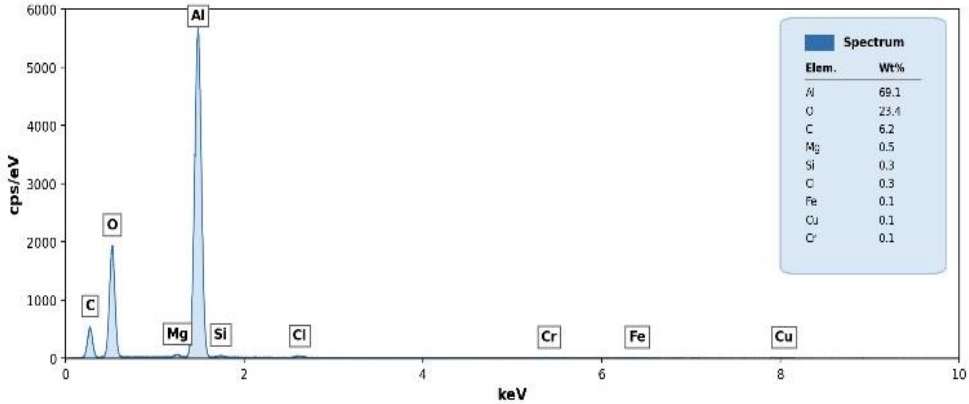

Figure 10. Energy-dispersive X-ray spectroscopy (EDS) analysis of AA6061 alloy sample exposed to simulated formation water with 2.5% orange peel extract (OPE) concentration at 50 ℃

However, the 2.5% OPE solution at 25 ℃ yielded an increased amount of carbon ions and decreased chloride ions on the aluminum surface, which supports the adsorption of organic molecules from the inhibitor and the formation of a protective film on the aluminum surface. Similarly, the 2.5% OPE solution at 50 ℃ had a lower amount of carbon ions than at 25 ℃, indicating that the adsorption process became unstable when the temperature increased.

3.7 Inhibition mechanism

Considering the electrochemical and surface analyses performed, it is likely that the adsorption mechanisms are vital to the performance of the AA6061 OPE inhibitor. Indeed, the decrease in the Icorr and CR, together with the increased inhibition efficiency (IE%), indicate that OPE significantly suppresses the rate of electrochemical processes occurring at the metal/solution interface. It should be noted that various phytochemical components in the extract, such as polyphenols, organic acids, and oxygen-containing functional groups (hydroxyl, carboxyl, and carbonyl groups), play pivotal roles in the adsorption process. The presence of these functional groups was confirmed by FTIR spectroscopy. The molecules containing these groups undergo an adsorption process based on donor-acceptor interactions between the lone pair electrons/π-electrons and empty aluminum orbitals. Consequently, a protective adsorption film was formed. SEM and EDS studies have also shown the formation of such an anticorrosive film. More specifically, corroded AA6061 surfaces without an inhibitor showed significant levels of pitting. Moreover, there was a noticeable increase in the amount of carbon and a decrease in the amount of chloride found on the surfaces of the aluminum that were inhibited by OPE, which means that an organic coating developed on the metallic surfaces. Therefore, it can be assumed that the OPE provides protection by developing a protective film that covers the metallic surface and prevents aggressive chloride ions present in the solution from accessing the metal surface. The effect of temperature further supports the proposed mechanism of corrosion inhibition, as only a decrease in inhibition efficiency was observed when the temperature increased. This observation suggests that physisorption may significantly contribute to the adsorption behavior (because it is highly temperature sensitive). Nevertheless, some chemical interactions are expected because of the presence of polar functional groups that can undergo coordinate bonding. Finally, the relatively minor change in corrosion potential (Ecorr) during polarization studies shows that OPE is a mixed-type inhibitor that reduces both anodic and cathodic reactions, but does not affect the corrosion process in any way. Regarding the practical application of these results, based on the inhibition behavior obtained, it can be assumed that OPE can efficiently adhere to the AA6061 surface and create a protective layer of inhibitor molecules under the studied experimental conditions. According to the results obtained, OPE can effectively act as a corrosion inhibitor when injected into certain systems.

A small decrease in the effectiveness of inhibition was recorded when the highest concentration of OPE was used. This phenomenon can be caused by the change in the adsorption properties of an inhibitor molecule at high concentrations. One possibility is that an excessive number of molecules leads to destabilization of the adsorbed layer. Nevertheless, it is worth noting that owing to the absence of electrochemical impedance spectroscopy (EIS) and X-ray photoelectron spectroscopy (XPS) measurements, as well as EDS measurements for the 3% solution, this is only an assumption.

4. CONCLUSIONS

The inhibitory behavior of OPE on AA6061 in synthetic formation water was analyzed in this study. Electrochemical studies showed a marked decrease in Icorr and CR with increasing OPE concentration, attaining a maximum inhibition efficiency of 98.99% at 2.5%. In terms of temperature dependency, it was observed that the corrosion activity increased with an increase in temperature; however, the efficacy of the OPE remained relatively high despite slight degradation attributed to desorption effects. Infrared spectroscopy analysis indicated the presence of oxygen-bearing functional groups (-OH, C =O, and C-O), which facilitated adsorption on the metal surface. Surface morphology studies using SEM illustrated an improved surface morphology, suggesting that a protective adsorbed layer was formed. It can be concluded that adsorption plays a major role in the inhibition process and contributes to the formation of a protective barrier film, which results in the formation of a protective barrier film.

5. LIMITATIONS OF THE STUDY

Potentiodynamic polarization, FTIR, and SEM were used in the current study to examine the inhibition properties of orange peel extract towards corrosion. Although such methods yield useful data concerning the efficacy of inhibitors and their adsorption on the surface, they do not allow us to draw concrete conclusions about the type of adsorption process. Further research involving EIS the study of adsorption equilibrium, and thermodynamic calculations is highly recommended.

ACKNOWLEDGMENT

The authors would like to extend their sincere thanks to Mustansiriyah University for its constant support and provision of the required equipment for conducting the present study. We are also thankful for the extended cooperation of the technical staff during the completion of this study.

REFERENCES

[1] Abdulrehman, M.A., Challoob, S.H., Marhoon, I.I. (2020). Investigation of mechanical and numerical properties of friction stir welding (FSW) for 3003-H14 aluminum alloys. Defect and Diffusion Forum, 398: 106-116. https://doi.org/10.4028/www.scientific.net/DDF.398.106

[2] Al-Amiery, A.A., Yousif, E., Wan Isahak, W.N.R., Al-Azzawi, W.K. (2023). A review of inorganic corrosion inhibitors: Types, mechanisms, and applications. Tribology in Industry, 45(2): 313-339. https://doi.org/10.24874/ti.1456.03.23.06

[3] Wang, X.X., Chen, L., Yang, F., Xiang, Q., Liu, J. (2023). Corrosion inhibition mechanism and extraction technology of plant corrosion inhibitors: A review. Journal of Adhesion Science and Technology, 37(21): 2919-2943. https://doi.org/10.1080/01694243.2023.2172993

[4] Prabu, B., Annadurai, S., Panneerselvam, S., Prabakaran, M., Kim, J. (2023). An outline of employing metals and alloys in corrosive settings with ecologically acceptable corrosion inhibitors. Surfaces, 6(4): 380-409. https://doi.org/10.3390/surfaces6040027

[5] Daniyal, M., Raja, M.A. (2016). Use of corrosion inhibitors for steel protection in cementitious composites-A review. International Journal of Advanced Engineering Research and Science, 3(6): 171-175.

[6] Phuyal, A., Poudel, M., Bhandari, R., et al. (2024). Phytochemical composition and corrosion inhibitory efficiency of Tinospora cordifolia and Senna alata plant extracts on mild steel in acidic media. Butwal Campus Journal, 7(2): 25-40. https://doi.org/10.3126/bcj.v7i2.73175

[7] Bilgiç, S. (2021). Plant extracts as corrosion inhibitors for mild steel in HCl media – Review I. International Journal of Corrosion and Scale Inhibition, 10(1): 145-175. https://doi.org/10.17675/2305-6894-2021-10-1-9

[8] Es'haghi, M., Amjad, A., Asghari, S., Lotfi, A. (2018). Studying effect of plantain extract behavior as an eco-friendly corrosion inhibitor on the mild steel in 1 M HCl solution. Anti-Corrosion Methods and Materials, 65(3): 310-316. https://doi.org/10.1108/ACMM-10-2017-1857

[9] Chaouiki, A., Chafiq, M., Ko, Y.G., et al. (2022). Adsorption mechanism of eco-friendly corrosion inhibitors for exceptional corrosion protection of carbon steel: Electrochemical and first-principles DFT evaluations. Metals, 12(10): 1598. https://doi.org/10.3390/met12101598

[10] Salam Abd Samar, A.E., Maksoud Abd Samar, A.E. (2017). Mitigation of corrosion of carbon steel in acid medium using some antipyrine derivatives. Zaštita Materijala, 58(1): 5-15. https://doi.org/10.5937/ZasMat1701005F

[11] Baloyi, T.H., Mashuga, M.E., El-Khlifi, A., Salman, M., Bahadur, I. (2025). Exploring the structural effects of benzaldehyde derivatives as corrosion inhibitors on mild steel in acidic medium using computational and experimental approaches. Corrosion and Materials Degradation, 6(3): 29. https://doi.org/10.3390/cmd6030029

[12] Omari, M., Bouiti, K., Jebbari, S., et al. (2025). Corrosion inhibition of C38 steel in 1 M HCl using benzoxazole-2-thione: Electrochemical, SEM-EDX, and theoretical studies. Metals, 15(7): 810. https://doi.org/10.3390/met15070810

[13] Pascoal, C.V.P., Da Silva, L.R.R., Florez, M.A.C., et al. (2025). Assessment of sustainable ethanolamine-based protic ionic liquids with varied carboxylic acid chains as corrosion inhibitors for carbon steel in saline environments. Molecules, 30(5): 1033. https://doi.org/10.3390/molecules30051033

[14] Adnan, Y., Ait Elmachkouri, Y., Idlahoussaine, N., Irrou, E., et al. (2025). Effectiveness of a novel C4-substituted heterocyclic organic pyrazolone as a corrosion inhibitor for mild steel in 1.0 M HCl: Electrochemical, surface analytical and theoretical studies. RSC Advances, 15(48): 40558-40573. https://doi.org/10.1039/D5RA03090K

[15] Kedimar, N., Rao, P., Rao, S.A. (2025). Evaluating the corrosion behavior of 6061 Al-10(vol.%) SiC(P) composite in varied HCl concentration using ionic liquid: Electrochemical and surface studies. Canadian Metallurgical Quarterly, 64(1): 162-175. https://doi.org/10.1080/00084433.2024.2306000

[16] Sun, K.T., Zhong, W.C., Huang, S.Q., et al. (2025). Research progress on the corrosion mechanism and protection monitoring of metal in power equipment. Coatings, 15(2): 119. https://doi.org/10.3390/coatings15020119

[17] Shi, Z.J., Fang, Q.H., Liaw, P.K., Li, J. (2023). Corrosion-resistant biomedical high-entropy alloys: A review. Advanced Engineering Materials, 25(22): 2300968. https://doi.org/10.1002/adem.202300968

[18] Milošev, I. (2019). Contemporary modes of corrosion protection and functionalization of materials. Acta Chimica Slovenica, 66(3): 511-533. https://doi.org/10.17344/acsi.2019.5162

[19] Policastro, S., Martín, F., Natishan, P., Moran, P. (2011). Corrosion and corrosion control. Kirk-Othmer Encyclopedia of Chemical Technology. https://doi.org/10.1002/0471238961.031518181315180 1.a01.pub3

[20] Timoudan, N., Al-Gorair, A.S., El Foujji, L., et al. (2024). Corrosion inhibition performance of benzimidazole derivatives for protection of carbon steel in hydrochloric acid solution. RSC Advances, 14(41): 30295-30316. https://doi.org/10.1039/d4ra05070c

[21] Abdulrehman, M.A., Hussein, M.A.M., Marhoon, I.I. (2022). Temperature-dependent mechanical properties of Al/Cu nanocomposites under tensile loading via molecular dynamics method. Curved and Layered Structures, 9(1): 96-104. https://doi.org/10.1515/cls-2022-0009